A R C H I V E O F M E C H A N I C A L E N G I N E E R I N G

Volume 68 2021 Number 2

DOI: 10.24425/ame.2021137045

Key words: hydrostatic lubrication, pressurized bearings, thrust bearings, surface roughness, cubic stress fluids

Udaya P. Singh [1]

Effect of surface roughness on steady performance of hydrostatic thrust bearings: Rabinowitsch fluids

The present theoretical study is concerned with the analysis of surface roughness effects on the steady-state performance of stepped circular hydrostatic thrust bearings lubricated with non-Newtonian fluids: Rabinowitsch fluid model. To take the effects of surface roughness into account, Christensen's theory for rough surfaces has been adopted. The expression for pressure gradient has been derived in stochastic form employing the energy integral approach. Results for stochastic film pressure and load-carrying capacity have been plotted and analyzed based on numerical results. Due to surface roughness, significant variations in the theoretical results of these properties have been observed.

Nomenclature

c	roughness parameter as defined after Eq. (5)
$E(.)$	expectancy function
$F(.)$	probability density function as taken in Eq. (3)
$\bar{h}, h$	nominal smooth part of film thickness, $h = \bar{h}/R$
$\bar{\hbar}, \hbar$	total film thickness, $\hbar = \bar{\hbar}/R$
$\bar{h}_s, h_s$	part of film thickness due to asperities, $h_s = \bar{h}_s/R$
p_o	supply pressure
$\bar{p}, p$	film pressure, $p = \bar{p}/p_o$
P	$E(p)$
$\bar{Q}, Q$	lubricant flow rate, $Q = \mu\bar{Q}/(p_o R^3)$
R	bearing radius
$\bar{r}, r$	variable in radial direction, $r = \bar{r}/R$
$\bar{r}_0, r_0$	radius of supply hole, $r_0 = \bar{r}_0/R$
$\bar{r}_1, r_1$	step position, $r_1 = \bar{r}_1/R$

✉ Udaya P. Singh, e-mail: journals4phd@gmail.com

[1] Rajkiya Engineering College, Sonbhadra, Uttar Pradesh, India. ORCID: 0000-0002-4538-9377

S	$\frac{3}{20}\frac{\rho R^2\Omega^2}{p_o}$ (inertia parameter)
$\bar{u}, u$	radial velocity, $u = \bar{u}/(R\Omega)$
$\bar{v}, v$	circumferential velocity, $v = \bar{v}/(R\Omega)$
$\overline{W}, W$	load capacity, $W = \frac{\overline{W}}{\pi R^2 p_o}$
$\bar{z}, z$	variable in Z-direction, $z = \bar{z}/R$
α	κp_o^2
β	film thickness ratio
κ	coefficient of pseudoplasticity
μ_0	zero shear rate viscosity of fluid
$\bar{\mu}, \mu$	viscosity of fluid, $\mu = \bar{\mu}/\mu_0$
$\bar{\tau}_{rz}, \tau_{rz}$	shear stress, $\tau_{rz} = \bar{\tau}_{rz}/p_o$

1. Introduction

Amongst the externally pressurized bearings, circular hydrostatic thrust bearings are of great importance for industrial and engineering applications due to their wide uses in high-speed rotating machines. Researchers have also paid significant attention to the improvement of the performance of these bearings under various operating and lubricating conditions [1–5]. Several investigations have been carried out to analyze the dependence of different performance properties of these bearings on rotational inertia, fluid compressibility, and temperature variation of the fluid [6–8]. Optimization of the design of hydrostatic thrust bearings with special consideration on shape and radii of recess and supply hole and different operating conditions have been done time-to-time [9–14]. Yadav and Kapur [15] considered the combined effect of temperature and inertia on the overall performance of hydrostatic step thrust bearings. Some investigators also focused their attention on analyzing the dynamic performance of hydrostatic thrust bearings lubricated with Newtonian and couple stress fluids [16, 17].

At the same time, many researchers also emphasized that surface roughness plays a very important role in the performance of lubricated bearings [18]. Prakash and Tiwari [19] presented the analysis of porous bearing with surface corrugations. Singh, Gupta and Kapur [20] studied the characteristics of corrugated thrust bearings. Lin [21] analyzed surface roughness effect on the dynamic stiffness and damping characteristics of compensated hydrostatic thrust bearings. Yacout, Ismaeel and Kassa [22] studied the combined effects of the centripetal inertia and the surface roughness on the hydrostatic thrust spherical bearings performance. Xuebing et al. [23] investigated the combined effect of the surface roughness and inertia on the performance of high-speed hydrostatic thrust bearing. Walicka et al. [24] analyzed various performance characteristics of thrust bearing with rough surfaces lubricated with non-Newtonian fluids by using Ellis fluid model.

Tribologists also worked to increase the stabilizing properties of non-Newtonian lubricants by the addition of long-chain polymer solutions (polyisobutylene and

ethylene-propylene etc.) as viscosity index improvers [25–27]. The use of additives reduces the sensitivity of the lubricant to the change in the shearing strain rate with temperature due to which the lubricant's characteristics deviate from that of Newtonian fluids [27]. To study the lubrication regimes with such lubricants, many non-Newtonian models such as couple stress, power law, micropolar, and Casson models are of common interest. Amongst these models, cubic stress (Rabinowitsch) fluid model [1–3] is an established model to analyze the non-Newtonian behavior of the fluid. Wada and Hayashi [26] showed that the lubricants blended with viscosity index improver behave like pseudoplastic fluids, which can be analyzed with cubic stress (Rabinowitsch) fluid model given by following relation for one-dimensional fluid flow:

$$\bar{\tau}_{rz} + \kappa \bar{\tau}_{rz}^3 = \bar{\mu} \frac{\partial \bar{u}}{\partial \bar{z}}, \tag{1}$$

where, $\bar{\mu}$ is the *initial viscosity* and κ is the non-linear factor responsible for the non-Newtonian effects of the fluid, which will be referred to as the coefficient of pseudoplasticity in this paper. This model applies to Newtonian lubricants ($\kappa = 0$), dilatant lubricants ($\kappa < 0$), and pseudoplastic lubricants ($\kappa > 0$). This model is one of the few models supported by experimental verification [26]. Many researchers used this model for the theoretical study of bearing performance with non-Newtonian lubricants [28–31]. Singh, Gupta and Kapur [32] analyzed the effects of inertia in the steady-state pressurized flow of a non-Newtonian fluid between two curvilinear surfaces of revolution. Lin [33] studied the squeeze film characteristics between parallel annular disks. Singh [34] and Singh, Gupta and Kapur [35, 36] investigated the effects of non-Newtonian pseudoplastic lubricants on the various performances of squeeze film, hydrodynamic sliders. Sharma and Yadav [37] presented the analysis of hydrostatic circular thrust pad bearing. Huang and Tian [38] also used Rabinowitsch fluid model to study pressure distribution and load capacity of hydrostatic thrust bearings. Recently, Singh, Sinha and Kumar [39] investigated the effects of inertia in the supply region on the pressure distribution and dependent characteristics of hydrostatic thrust bearings. In light of this discussion, it is observed that surface roughness and non-Newtonian lubricants are important considerations for the analysis of hydrostatic thrust bearings, and none of the researchers has analyzed the combined effects of surface roughness, inertia and non-Newtonian lubricants on hydrostatic thrust bearings. Furthermore, for theoretical analysis of a bearing, it is very crucial to select a rheological model that is valid for the defined flow field.

In the light of this discussion, it is proposed to investigate the combined effects of surface roughness, non-Newtonian fluids, and fluid inertia on the performance of a hydrostatic thrust bearing using cubic stress fluid model (an experimentally verified fluid model [26]), and thereby, extend the results of Singh, Gupta and Kapur [1].

2. Analysis

A schematic configuration of a hydrostatic thrust bearing with rough surfaces is shown in Fig. 1. It is assumed that the flow of lubricant between the bearing plates is laminar, the lubricant is incompressible non-Newtonian fluid, the body forces and body couples are absent, and the assumptions of hydrodynamic lubrication apply to lubricant film. Following Singh, Gupta and Kapur [1], the expression for pressure gradient is obtained as (cf. Appendix):

$$\frac{\partial p}{\partial r} = -\frac{1}{6\mu Q}\left[r\left(\hbar^3 f^2 + \frac{3\alpha}{20}\hbar^5 f^4\right) + \frac{3\Omega}{10}r^2\left(\hbar^3 f + \alpha f^3 \frac{13\hbar^5}{84}\right)\right], \tag{2}$$

where, $f = -\dfrac{6\mu Q}{r\hbar^3}\left(1 - \dfrac{27}{5}\dfrac{\alpha\mu^2 Q^2}{r^2\hbar^4}\right)$ and $\hbar = \beta h + h_s$. Here, r represent radial coordinate, h is the nominal smooth part of the film thickness, β is step ratio, h_s is the part of film thickness due to asperities on the surface measured from smooth level; all the quantities are in dimensionless form. In the case of radial roughness, $h_s = h_s(\theta, \xi)$, and in the case of transverse or circumferential roughness, $h_s = h_s(r, \xi)$; where, ξ is a random variable to characterize some definite arrangement of the surface asperities. The boundary conditions for Eq. (2) are: $p(r_0) = 1$ and $p(1) = 0$ together with the continuity of pressure at the step.

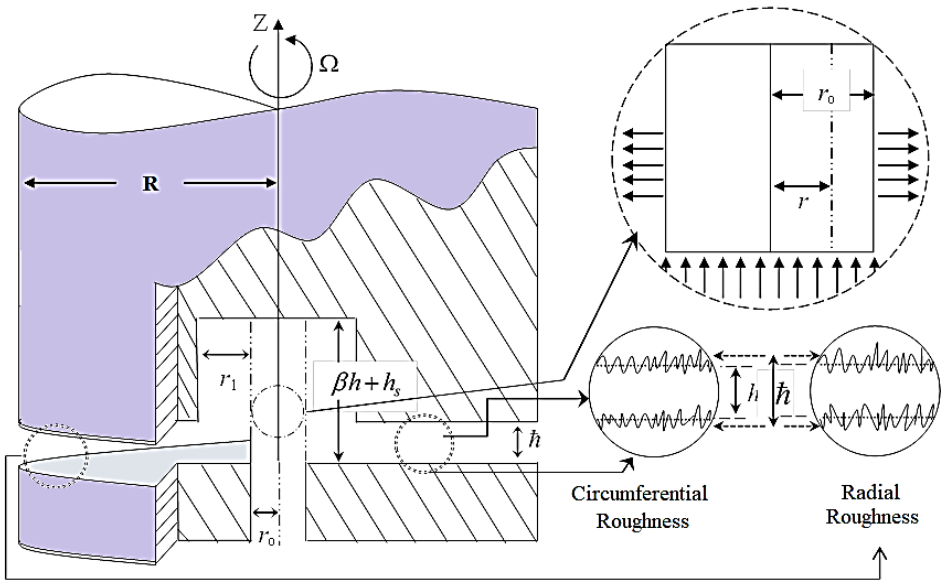

Fig. 1. Schematic diagram of step thrust bearing with rough surfaces

Taking the dimensionless probability density function of the stochastic film thickness $F(h_s)$, Christensen [18]:

$$F(h_s) = \begin{cases} \dfrac{35}{32c^7}\left(c^2 - h_s^2\right)^3, & -c < h_s < c, \\ 0, & \text{elsewhere} \end{cases} \tag{3}$$

and defining the expectancy function $E(\Theta)$ as:

$$E(\Theta) = \int_{-\infty}^{\infty} \Theta\, F(h_s)\, \mathrm{d}h_s\,, \tag{4}$$

the stochastic form of Eq. (2) can be written as:

$$\frac{\partial E(p)}{\partial r} = -\frac{1}{6\mu Q} E\left(\left[r\left(\hbar^3 f^2 + \frac{3\alpha}{20}\hbar^5 f^4\right) + \frac{3\Omega}{10} r^2 \left(\hbar^3 f + \alpha f^3 \frac{13\hbar^5}{84}\right)\right]\right), \tag{5}$$

where, c is the half range assumed by the random film thickness variable ξ with the standard deviation σ. The function $f(h_s)$ – defined in Eq. (3) terminates at $c = \pm 3\sigma$. In the present analysis, c will be referred to as roughness parameter.

Denoting stochastic film pressure $E(p)$ by P and integrating Eq. (5) with respect to r along the radius of the bearing, we obtain the following expression:

$$P(r) = 1 - \frac{1}{6\mu Q} \int_{r_0}^{r} E\left(\left[r\left(\hbar^3 f^2 + \frac{3\alpha}{20}\hbar^5 f^4\right) + \frac{3\Omega}{10} r^2 \left(\hbar^3 f + \alpha f^3 \frac{13\hbar^5}{84}\right)\right]\right) \mathrm{d}r, \tag{6}$$

where, the evaluation of integral on the right-hand side of Eq. (6) requires the exact expressions for expectation function occurring in the integrand.

The dimensionless load carrying capacity is calculated as:

$$W = 2\int_0^1 rP(r)\,\mathrm{d}r = r_0^2 + 2\int_0^{r_1} rP(r)\,\mathrm{d}r + 2\int_{r_1}^1 rP(r)\,\mathrm{d}r, \tag{7}$$

where, the quantities r_0 and r_1 represent relative radii of the supply hole and recess region, respectively.

Evaluation for volumetric flow rate (Q) has been done using Newton-Raphson method. Numerical values of Q, $P(r)$ and W have been obtained using *Mathematica 11.0*.

3. Pressure distribution

Case I: Radial roughness

For the radial roughness, the stochastic film thickness is $\hbar = \beta h + h_s(\theta, \xi)$ and stochastic form of Eq. (6) is

$$P(r) = 1 - \frac{1}{6\mu Q}\int_{r_0}^{r}\left[r\left(E(\hbar^3)E(f)^2 + \frac{3\alpha}{20}E(\hbar^5)E(f)^4\right) + \frac{3\Omega}{10}r^2\left(E(\hbar^3)E(f) + \alpha\frac{13E(\hbar^5)}{84}E(f)^3\right)\right]\mathrm{d}r, \tag{8}$$

where,

$$E(f) = -\frac{6\mu Q}{r}\left(\frac{1}{E(\hbar^3)} - \frac{27}{5}\frac{\alpha\mu^2Q^2}{r^2E(\hbar^7)}\right), \tag{9}$$

$$E\left(\hbar^3\right) := \frac{1}{3}c^2h\beta + h^3\beta^3, \tag{10}$$

$$E\left(\hbar^5\right) := \frac{5}{33}c^4h\beta + \frac{10}{9}c^2h^3\beta^3 + h^5\beta^5, \tag{11}$$

$$E\left(\hbar^7\right) := \frac{35}{429}c^6h\beta + \frac{35}{33}c^4h^3\beta^3 + \frac{7}{3}c^2h^5\beta^5 + h^7\beta^7. \tag{12}$$

Equtions (8)–(12) represent the expression for pressure in the case of radial roughness, which gives the pressure in the recess region ($r_0 \leqslant r \leqslant r_1$) for $\beta \neq 1$, and pressure in the land region ($r_1 \leqslant r \leqslant 1$) for $\beta = 1$.

Case II: Circumferential or azimuthal roughnes

For the circumferential roughness, the stochastic film thickness is $\hbar = \beta h + h_s(r, \xi)$ and stochastic form of Eq. (6) is

$$P(r) = 1 - \frac{1}{6\mu Q}\int_{r_0}^{r}\left[r\left(\frac{E(f)^2}{E(\hbar^{-3})} + \frac{3\alpha}{20}\frac{E(f)^4}{E(\hbar^{-5})}\right) + \frac{3\Omega}{10}r^2\left(\frac{E(f)}{E(\hbar^{-3})} + \alpha\frac{13}{84}\frac{E(f)^3}{E(\hbar^{-5})}\right)\right]\mathrm{d}r, \tag{13}$$

where,

$$E(f) = -\frac{6\mu Q}{r}\left(E(\hbar^{-3}) - \frac{27}{5}\frac{\alpha\mu^2Q^2}{r^2}E(\hbar^{-7})\right), \tag{14}$$

$$E\left(\hbar^{-3}\right) = \frac{35}{32c^7}\left(3\left(6c^2h^2\beta^2 - c^4 - 5h^4\beta^4\right)\log\left(\frac{h\beta+c}{h\beta-c}\right) + 30ch^3\beta^3 - 26c^3h\beta\right), \tag{15}$$

$$E\left(\hbar^{-5}\right)=\frac{35}{32}\frac{3\left(c^4-6c^2h^2\beta^2+5h^4\beta^4\right)\log\left(\frac{h\beta+c}{h\beta-c}\right)+26c^3h\beta-30ch^3\beta^3}{c^7\left(c^2-h^2\beta^2\right)}, \tag{16}$$

$$E\left(\hbar^{-7}\right)=-\frac{7}{96}\frac{15\left(c^2-h^2\beta^2\right)^3\log\left(\frac{h\beta+c}{h\beta-c}\right)-80c^3h^3\beta^3+66c^5h\beta+30ch^5\beta^5}{c^7\left(c^2-h^2\beta^2\right)^3}. \tag{17}$$

Equtions (13)–(17) give the pressure in the recess region ($r_0 \leqslant r \leqslant r_1$) for $\beta \neq 1$, and land region ($r_1 \leqslant r \leqslant 1$) for $\beta = 1$.

4. Results and discussion

In order to analyze the effect of roughness on the steady-state performance characteristics of externally pressurized thrust bearings lubricated with non-Newtonian (pseudoplastic) lubricants, numerical results for stochastic values of pressure and load capacity have been obtained for the different values of roughness parameter c ($0 \leqslant c \leqslant 0.005$) and the parameter of pseudoplasticity, α ($\alpha = \kappa P_o^2$). For the practical justification, results have been discussed for the experimental values for coefficient of pseudoplasticity, $\kappa = 5.65 \cdot 10^{-6}$ m^4/N^2 (0.3% additive) and $3.05 \cdot 10^{-6}$ m^4/N^2 (1% additive) have been taken [26] (Table 1). The values of operating parameters, namely, film thickness ratio $\beta = 2, 5$; parameter of centrifugal inertia $S = 0, 1.0, 2.0$; supply radius $r_0 = 0.05$, and step radius $r_1 = 0.4$ have been taken from experimental results of Dowson [6] (Table 2). Further, the theoretical

Table 1.

Lubricants additive*

Additives (%)	T (°C)	μ (Pa·s)	κ (m^4/N^2)
0	25	0.140	0×10^{-6}
0.3	22	0.250	5.65×10^{-6}
1.0	22	0.610	3.05×10^{-6}
2.0	25	0.865	2.95×10^{-6}

* Data taken from experimental result of Wada and Hayashi [26]

Table 2.

Supply pressure#

β	$\bar{r}_0$ (m)	$\bar{r}_1$ (m)	$\bar{h}$ (m)	P_0 (N/m^2)
1.54	0.00675	0.0254	0.000424	13513
2.18	0.00675	0.0254	0.0001715	20271

Data taken from experimental result of Coombs and Dowson [6]

results of pressure for Newtonian and non-Newtonian (pseudoplastic) lubricants have been compared with the experimental results of Dowson [6], and the results for both load capacity and pressure have been compared with the established theoretical results of Singh, Gupta and Kapur [1]. It was observed that pressure and load capacity for smooth surfaces ($c = 0$) in the present analysis are the same as those obtained by Singh, Gupta and Kapur [1].

Fig. 2 shows the variation of film pressure along the radial direction for film thickness ratio $\beta = 2.18$ and different values of roughness parameter (c), coefficient of pseudoplasticity (κ) and inertia parameter (S). To maintain the graphical clarity, the results for longitudinal and circumferential roughness have been presented as separate figures. In both the case of longitudinal and circumferential roughness patterns, the dimensionless pressure for $c = 0$ is the same as obtained by Singh, Gupta and Kapur [1] for each value of S, which validates the present results for smooth surfaces. It is, further, observed that the longitudinal roughness decreases the dimensionless values of film pressure, while the circumferential roughness pattern increases the dimensionless pressure. In the case of the longitudinal roughness patterns ($c = 0.005$), the pressure is lower than that for $c = 0$ in both the cases of Newtonian as well as non-Newtonian lubricants, and the trend holds for each value of $S = 0$, 1 and 2, while the case is reversed in case of circumferential roughness patterns. Further, in comparison to smooth surface, the theoretical values of pressure obtained for rough surfaces with longitudinal roughness are closer to the experimental values. The pressure for longitudinal roughness ($c = 0.005$) and non-Newtonian lubricants $\kappa = 5.65 \cdot 10^{-6}$ are more close to the experimental results [6] than the theoretical results [1]. In Fig. 3, similar variation of profile of dimensionless pressure has been obtained and compared with the established theoretical and experimental results for film thickness $\beta = 1.54$. This establishes the sustainability of the present results of film pressure for surface roughness. Furthermore, all the figures for pressure also show that the effects of surface roughness and non-Newtonian lubricants are more significant at higher values of the inertia parameter S.

The variation in film pressure (Figs. 2, 3) due to the nature of roughness is physically consistent because, in the case of radial roughness, asperity ridges and valleys run in the direction of fluid flow. This facilitates the flow of lubricant through the valleys in the radial direction. Whereas for circumferential roughness, ridges and valleys run perpendicular to the direction of radial flow which restrict the easy flow of the lubricant (because the lubricant has to go over the ridges into the valleys and then rise again). This causes an increase in film pressure as compared to the case of radial roughness. Further, the pressure variation due to roughness is more dominant for higher values of β (Figs. 2), which is again consistent with the physical phenomenon because the higher step ratio causes cavitation in the land region which is reduced by the surface roughness.

Fig. 4 shows variation of dimensionless load capacity for the step position r_1 for different values of roughness parameter (c), coefficient of pseudoplasticity (κ)

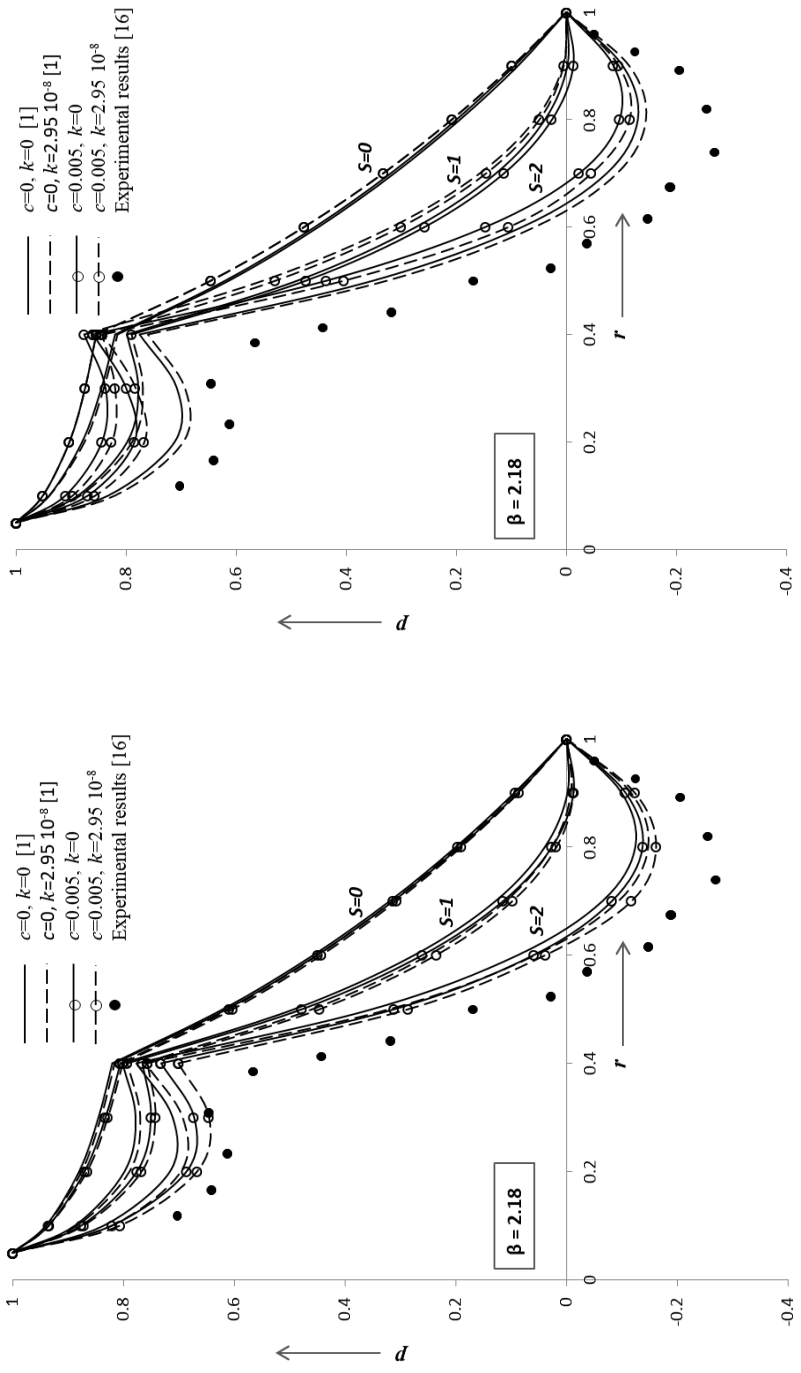

(a) results for longitudinal roughness

(b) results for circumferential roughness

Fig. 2. Variation of film pressure with radius for different values of inertia parameter (S) and roughness parameter (c)

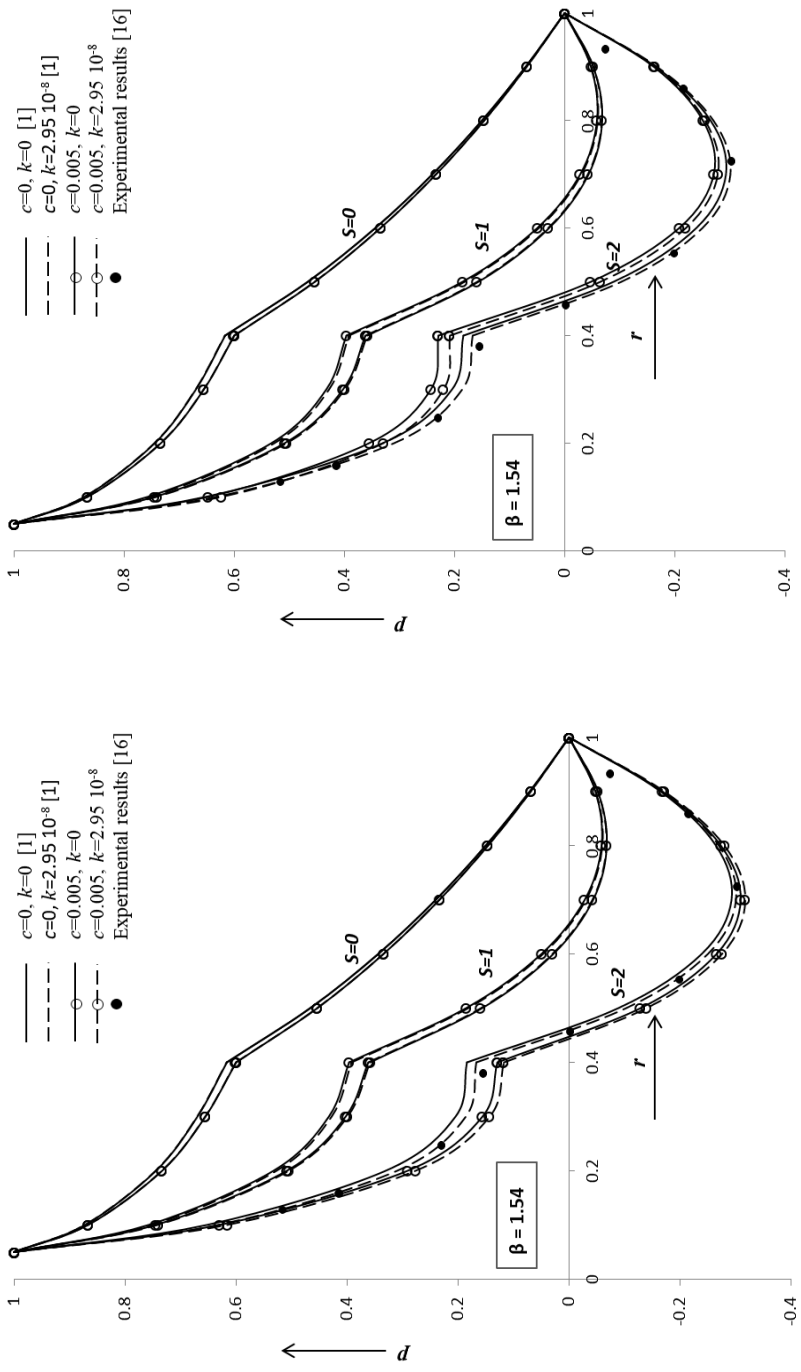

(a) results for longitudinal roughness (b) results for circumferential roughness

Fig. 3. Variation of film pressure with radius for different values of inertia parameter (S) and roughness parameter (c)

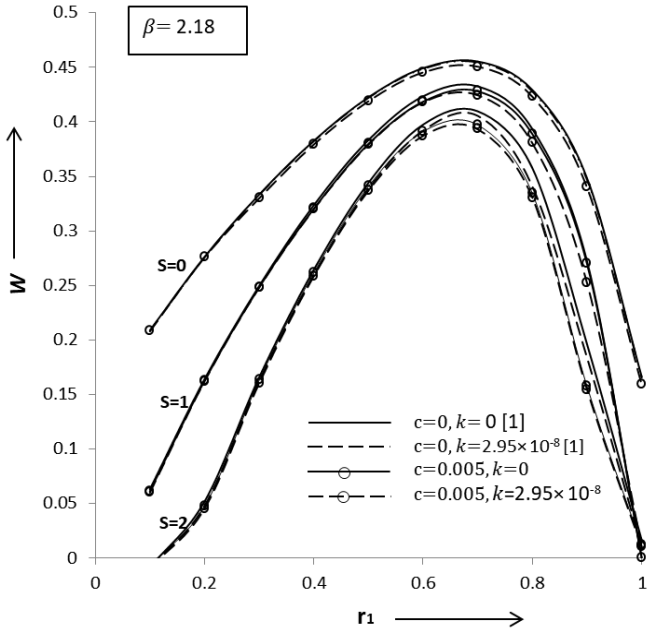

(a) results for longitudinal roughness

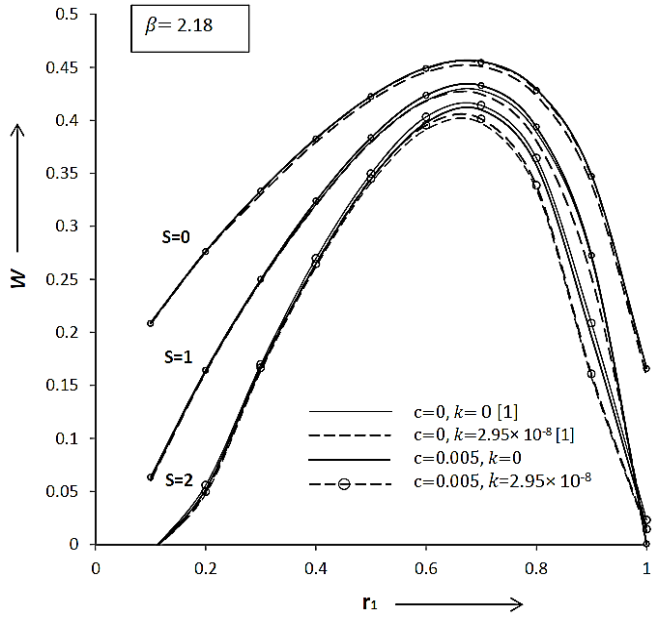

(b) results for circumferential roughness

Fig. 4. Variation of load capacity with step parameter (r_1) for different values of roughness parameter (c), inertia parameter S and coefficient of pseudoplasticity κ

and inertia parameter (S). In the case of smooth surfaces ($c = 0$), the load capacity obtained in the present analysis is the same as that obtained by Singh, Gupta and Kapur [1] for each value of $S = 0$, 1 and 2. The load capacity for surface with longitudinal roughness pattern ($c = 0.005$) is smaller than that for smooth surfaces in both the cases of Newtonian and non-Newtonian lubricants, and the trend of variations sustain for each value of S. In the case of circumferential roughness patterns, the results are reversed. Furthermore, it can be observed from the figures that higher is the value of inertia parameter S, more significant are the effects of surface roughness and non-Newtonian lubricants.

Fig. 5 shows the variation of load carrying capacity with roughness parameters (c) for inertia parameter ($S = 0, 1, 2$), Newtonian lubricants ($\kappa = 0$), pseudoplastic lubricants ($\kappa = 2.95 \cdot 10^{-8}$) and a typical value of step parameter $r_1 = 0.4$. Results for both the type of longitudinal and circumferential roughness patterns are plotted simultaneously to observe the influence of surface roughness and its pattern on the load capacity more precisely. It is easy to observe that load carrying capacity decreases with the increase of longitudinal roughness and increases with the increase of circumferential roughness for Newtonian as well as pseudoplastic lubricants at each value of the inertia parameter S. It is also clearly observed that surface roughness has a more significant influence on load capacity for higher values of the inertia parameter S.

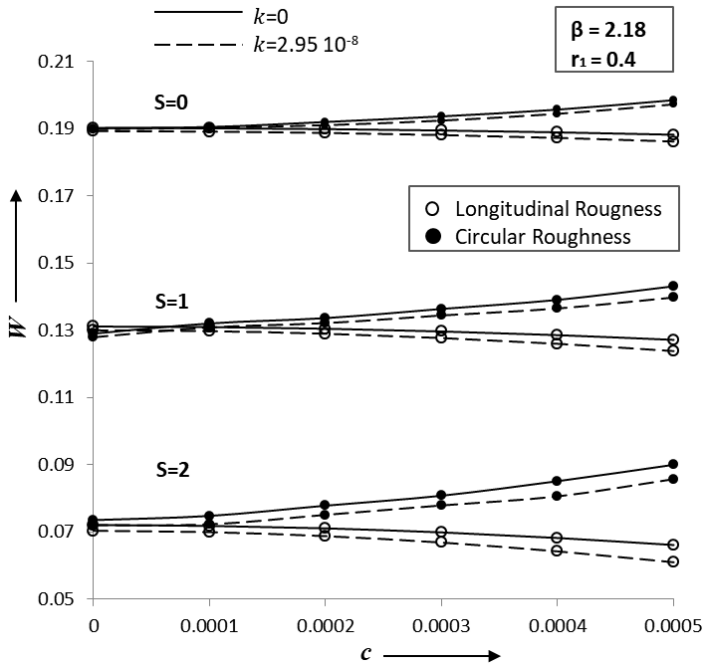

Fig. 5. Variation of load capacity with roughness parameter (c) for different values of inertia parameter S and coefficient of pseudoplasticity κ

4.1. Numerical example

Let us take a plane circumferential hydrostatic thrust bearing with the specifications: radius ($R = 0.27$ m), supply radius ($\bar{r}_0 = 0.0135$ m, recess radius ($\bar{r}_1 = 0.108$ m, nominal film thickness ($\bar{h} = 10^{-4}$ m, film thickness ratio ($\beta = 2.18$), rotor speed ($\Omega = 2700$ rpm, mean supply pressure $E(\bar{p}) = 20270$ Pa, initial viscosity of lubricant ($\mu_0 = 0.14$ Pa·s, viscosity of additive based lubricant $\overline{\mu} = 0.25$ Pa·s (0.3% additive), $\kappa = 5.65 \cdot 10^{-6}$ m^4/N^2 (0.3% additive), fluid density $\rho = 916$ kg/m^3 (approx.) and roughness measure 32 μm c.l.a. With this data, the inertia parameter is calculated as $S = 0.061$ and, the load capacity for

- smooth surface and Newtonian lubricant ($\overline{W} = 117.63$ Pa).
- smooth surface and additive (0.3%) based lubricant ($\overline{W} = 116.92$ Pa; relative change in load capacity = 0.602%.
- rough surface (32 μm c.l.a. Radial pattern) and additive (0.3%) based lubricant ($\overline{W} = 116.64$ Pa); relative change in load capacity = 0.848%.
- rough surface (32 μm c.l.a. circumferential pattern) and additive (0.3%) based lubricant ($\overline{W} = 118.68$ Pa; relative change in load capacity = 0.896%.

4.2. Limitations of the model

The present theoretical analysis is based on and valid under certain assumptions applicable to thin-film lubrication such as incompressible non-Newtonian fluid, no body forces and body couples, and laminar flow of lubricant. Furthermore, the analysis is also valid for a limited range of shear rates for which the Rabinowitsch model works. However, the present analysis can be always used to form a basic idea of the discussed characteristics, such as variation of pressure, load, and flow rate on the considered parameters.

5. Conclusions

Combined effects of surface roughness, non-Newtonian pseudoplastic lubricants, and lubricant inertia on the steady performance of hydrostatic thrust bearings, neglecting the radial inertia of lubricant and cavitation effects, have been presented. Cubic stress-strain model for non-Newtonian nature of the fluid, Christensen theory for surface roughness and *energy integral method* to derive pressure gradient were used in the analysis, based on which, the following conclusions are drawn

- In comparison with smooth surfaces, dimensionless film pressure and load capacity are lower for longitudinal roughness and higher for circumferential roughness patterns with Newtonian as well as non-Newtonian lubricants.
- In the case of longitudinal roughness patterns, load-carrying capacity decreases with increased roughness; and in the case of circumferential roughness, the load capacity increases with the increased roughness.

- In comparison with Newtonian lubricants, dimensionless pressure and load are lower for pseudoplastic lubricants, which is also the established result [1].
- Effects of surface roughness and non-Newtonian lubricants become more significant for larger values of inertia parameter, that is, for larger bearing radius and higher operating speed.

Hence, the present analysis is expected to be helpful for the theoretical approximation of plane circumferential hydrostatic thrust bearings.

A. Appendix

In absence of external body forces, the Navier-Stokes' equations for incompressible fluids can be represented in cylindrical polar coordinate system as:

$$\rho\left(\bar{u}\frac{\partial\bar{u}}{\partial\bar{r}}+\frac{\bar{v}}{\bar{r}}\frac{\partial\bar{u}}{\partial\theta}+\bar{w}\frac{\partial\bar{u}}{\partial\bar{z}}-\frac{\bar{v}^2}{\bar{r}}\right)=-\frac{\partial\bar{p}}{\partial\bar{r}}+\left(\frac{\partial\bar{\tau}_{rr}}{\partial\bar{r}}+\frac{1}{\bar{r}}\frac{\partial\bar{\tau}_{r\theta}}{\partial\theta}+\frac{\partial\bar{\tau}_{rz}}{\partial\bar{z}}\right), \tag{18}$$

$$\rho\left(\bar{u}\frac{\partial\bar{v}}{\partial\bar{r}}+\frac{\bar{v}}{\bar{r}}\frac{\partial\bar{v}}{\partial\theta}+\bar{w}\frac{\partial\bar{v}}{\partial\bar{z}}+\frac{\bar{u}\,\bar{v}}{\bar{r}}\right)=-\frac{1}{\bar{r}}\frac{\partial\bar{p}}{\partial\theta}+\left(\frac{\partial\bar{\tau}_{\theta r}}{\partial\bar{r}}+\frac{1}{\bar{r}}\frac{\partial\bar{\tau}_{\theta\theta}}{\partial\theta}+\frac{\partial\bar{\tau}_{\theta z}}{\partial\bar{z}}\right), \tag{19}$$

$$\rho\left(\bar{u}\frac{\partial\bar{w}}{\partial\bar{r}}+\frac{\bar{v}}{\bar{r}}\frac{\partial\bar{w}}{\partial\theta}+\bar{w}\frac{\partial\bar{w}}{\partial\bar{z}}\right)=-\frac{\partial\bar{p}}{\partial\bar{z}}+\left(\frac{\partial\bar{\tau}_{zr}}{\partial\bar{r}}+\frac{1}{\bar{r}}\frac{\partial\bar{\tau}_{z\theta}}{\partial\theta}+\frac{\partial\bar{\tau}_{zz}}{\partial\bar{z}}\right) \tag{20}$$

and the equation of continuity can be written as:

$$\frac{1}{\bar{r}}\frac{\partial}{\partial\bar{r}}\left(\bar{r}\,\bar{u}\right)+\frac{1}{\bar{r}}\frac{\partial\bar{v}}{\partial\theta}+\frac{\partial\bar{w}}{\partial\bar{z}}=0. \tag{21}$$

Under the assumptions of thin film lubrication [40] and radial symmetry of flow as applicable in present case, Eqs. (18)–(21) can be simplified to:

$$-\frac{\rho\bar{v}^2}{\bar{r}}=-\frac{\partial\bar{p}}{\partial\bar{r}}+\frac{\partial\bar{\tau}_{rz}}{\partial\bar{z}}, \tag{22}$$

$$0=\frac{\partial^2\bar{v}}{\partial\bar{z}^2}, \tag{23}$$

$$0=\frac{\partial\bar{p}}{\partial\bar{z}}, \tag{24}$$

$$\frac{1}{\bar{r}}\frac{\partial}{\partial\bar{r}}\left(\bar{r}\,\bar{u}\right)+\frac{\partial\bar{w}}{\partial\bar{z}}=0. \tag{25}$$

System of Eqs. (22)–(25) are solved under the conditions $\bar{u}=0$, $\bar{w}=0$ at $\bar{z}=0,\bar{h}$; $\bar{v}=0$ at $\bar{z}=0$; $\bar{v}=R\Omega$ at $\bar{z}=\bar{h}$; $\bar{p}=p_o$ at $\bar{r}=\bar{r}_0$ and $\bar{p}=0$ at $\bar{r}=R$.

With the dimensionless quantities

$$\alpha=\kappa p_o^2,\quad \tau_{rz}=\frac{\bar{\tau}_{rz}}{p_o},\quad \mu=\frac{\bar{\mu}}{\mu_0},\quad v=\frac{\bar{v}}{R\Omega},$$

$$u = \frac{\bar{u}}{R\Omega}, \quad z = \frac{\bar{z}}{R}, \quad r = \frac{\bar{r}}{R}, \quad p = \frac{\bar{p}}{p_o}, \quad S = \frac{3}{20}\frac{\rho R^2 \Omega^2}{p_o}.$$

Eq. (1) and Eqs. (22)–(25) are transformed to dimensionless form:

$$\tau_{rz} + \alpha \tau_{rz}^3 = \mu \frac{\partial u}{\partial z}, \tag{26}$$

$$-\frac{20}{3}\frac{Sv^2}{r} = -\frac{\partial p}{\partial r} + \frac{\partial \tau_{rz}}{\partial z}, \tag{27}$$

$$0 = \frac{\partial^2 v}{\partial z^2}, \tag{28}$$

$$0 = \frac{\partial p}{\partial z}, \tag{29}$$

$$\frac{1}{r}\frac{\partial}{\partial r}(r\,u) + \frac{\partial w}{\partial z} = 0. \tag{30}$$

The dimensionless boundary conditions are: $u = 0$, $w = 0$ at $z = 0, \hbar$; $v = 0$ at $z = 0$; $v = 1$ at $z = \hbar$; $p = 1$ at $r = r_0$ and $p = 0$ at $r = 1$.

Defining the volumetric flow rate as $\bar{Q} = 2\pi \int_0^{\bar{\hbar}} \bar{r}\,\bar{u}\,\mathrm{d}\bar{z}$ and taking $Q = \mu\bar{Q}/(p_o R^3)$, a close form solution (2) of Eq. (26)–(27) satisfying Eq. (30) can be easily obtained with energy integral method [1].

Manuscript received by Editorial Board, July 12, 2020;
final version, April 16, 2021.

References

[1] U.P. Singh, R.S. Gupta, and V.K. Kapur. On the steady performance of hydrostatic thrust bearing: Rabinowitsch fluid model. *Tribology Transactions*, 54(5):723–729, 2011. doi: 10.1080/10402004.2011.597541.

[2] U.P. Singh, R.S. Gupta, and V.K. Kapur. On the application of Rabinowitsch fluid model on an annular ring hydrostatic thrust bearing. *Tribology International*, 58:65–70, 2013. doi: 10.1016/j.triboint.2012.09.014.

[3] U.P.. Singh, R.S. Gupta, and V.K. Kapur. On the steady performance of annular hydrostatic thrust bearing: Rabinowitsch fluid model. *Journal of Tribology*, 134(4):044502, 2012. doi: 10.1115/1.4007350.

[4] B.J. Hamrock, S.R. Schmid, and B.O. Jacobson. *Fundamentals of Fluid Film Lubrication*. CRC Press, 2004. doi: 10.1201/9780203021187.

[5] R. Bassani and P. Piccigallo. *Hydrostatic Lubrication*, Elsevier, 1992.

[6] J.A. Coombs and D. Dowson. An experimental investigation of the effects of lubricant inertia in a hydrostatic thrust bearing. *Proceedings of the Institution of Mechanical Engineers, Conference Proceedings*, 179(10):96–114, 1964. doi: 10.1243/PIME_CONF_1964_179_270_02.

[7] J. Peterson, W.E. Finn, and D.W. Dareing. Non-Newtonian temperature and pressure effects of a lubricant slurry in rotating hydrostatic step bearing. *Tribology Transactions*, 37(4):857–863, 1994. doi: 10.1080/10402009408983369.

[8] V.K. Kapur and K. Verma. The simultaneous effects of inertia and temperature on the performance of a hydrostatic thrust bearing. *Wear*, 54(1):113–122, 1979. doi: 10.1016/0043-1648(79)90050-4.

[9] P. Singh, B.D. Gupta, and V.K. Kapur. Design criteria for stepped thrust bearings. *Wear*, 89(1):41–55, 1983. doi: 10.1016/0043-1648(83)90213-2.

[10] S.C. Sharma, S.C. Jain, and D.K. Bharuka. Influence of recess shape on the performance of a capillary compensated circular thrust pad hydrostatic bearing. *Tribology International*, 35(6):347–356, 2002. doi: 10.1016/S0301-679X(02)00013-0.

[11] Z. Tian, H. Cao, and Y. Huang. Static characteristics of hydrostatic thrust bearing considering the inertia effect on the region of supply hole. *Proceedings of the Institution of Mechanical Engineers, Part J: Journal of Engineering Tribology*, 233(1):188-193, 2019. doi: 10.1177/1350650118773944.

[12] Y.K. Younes. A revised design of circular hydrostatic bearings for optimal pumping power. *Tribology International*, 26(3):195–200, 1993. doi: 10.1016/0301-679X(93)90093-G.

[13] O.J. Bakker and R.A.J. van Ostayen. Recess depth optimization for rotating, annular, and circular recess hydrostatic thrust bearings. *Journal of Tribology*, 132(1):011103, 2010. doi: 10.1115/1.4000545.

[14] H. Sawano, Y. Nakamura, H. Yoshioka, and H. Shinno. High performance hydrostatic bearing using a variable inherent restrictor with a thin metal plate. *Precision Engineering*, 41:78–85, 2015. doi: 10.1016/j.precisioneng.2015.02.001.

[15] J.S. Yadav and V.K. Kapur. On the viscosity variation with temperature and pressure in thrust bearing. *International Journal of Engineering Science*, 19(2):269–77, 1981. doi: 10.1016/0020-7225(81)90027-6.

[16] P. Zhicheng, S. Jingwu, Z. Wenjie, L. Qingming, and C. Wei. The dynamic characteristics of hydrostatic bearings. *Wear* 166(2):215–220, 1993. doi: 10.1016/0043-1648(93)90264-M.

[17] J.R. Lin. Static and dynamic characteristics of externally pressurized circular step thrust bearings lubricated with couple stress fluids. *Tribology International*, 32(4):207–216, 1999. doi: 10.1016/S0301-679X(99)00034-1.

[18] H. Christensen. Stochastic models for hydrodynamic lubrication of rough surfaces. *Proceedings of the Institution of Mechanical Engineers*, 184(1):1013–1026, 1969. doi: 10.1243/PIME_PROC_1969_184_074_02.

[19] J. Prakash and K. Tiwari. Effect of surface roughness on the squeeze film between rotating porous annular discs with arbitrary porous wall thickness. *International Journal of Mechanical Sciences*, 27(3):135–144, 1985. doi: 10.1016/0020-7403(85)90054-2.

[20] P. Singh, B.D. Gupta, and V.K. Kapur. Optimization of corrugated thrust bearing characteristics. *Wear*, 167(2):109–120, 1993. doi: 10.1016/0043-1648(93)90315-D.

[21] J.R. Lin. Surface roughness effect on the dynamic stiffness and damping characteristics of compensated hydrostatic thrust bearings. *International Journal of Machine Tools and Manufacture*, 40(11):1671–1689, 2000. doi: 10.1016/S0890-6955(00)00012-2.

[22] A.W. Yacout. The surfacse roughness effect on the hydrostatic thrust spherical bearings performance: Part 3 of 5 – Recessed clearance type of bearings. In *Proceedings of the ASME International Mechanical Enginering Congress and Exposition, Volume 9: Mechanical Systems and Control, Parts A, B, and C*, pages 431–447, Seattle, Washington, USA, November 11–15, 2007. doi: 10.1115/IMECE2007-41013.

[23] Y. Xuebing, X. Wanli, L. Lang, and H. Zhiquan. Analysis of the combined effect of the surface roughness and inertia on the performance of high-speed hydrostatic thrust bearing. In: Luo J., Meng Y., Shao T., Zhao Q. (eds): *Advanced Tribology*, 197–201, Springer, 2009. doi: 10.1007/978-3-642-03653-8_66.

[24] A. Walicka, E. Walicki, P. Jurczak, and J. Falicki. Thrust bearing with rough surfaces lubricated by an Ellis fluid. *International Journal of Applied Mechanics and Engineering*, 19(4):809–822, 2014. doi: 10.2478/ijame-2014-0056.

[25] V.K. Stokes. Couple stress in fluids. *The Physics of Fluids*, 9(9):1709–1715, 1966. doi: 10.1063/1.1761925.

[26] S. Wada and H. Hayashi. Hydrodynamic lubrication of journal bearings by pseudo-plastic lubricants: Part 2, Experimental studies. *Bulletin of JSME*, 14(69):279–286, 1971. doi: 10.1299/jsme1958.14.279.

[27] H.A. Spikes. The behaviour of lubricants in contacts: current understanding and future possibilities. *Proceedings of the Institution of Mechanical Engineers, Part J: Journal of Engineering Tribology*, 208(1):3–15, 1994. doi: 10.1243/PIME_PROC_1994_208_345_02.

[28] P. Bourging and B. Gay. Determination of the load capacity of finite width journal bearing by finite element method in the case of a non-Newtonian lubricant. *Journal of Tribology*, 106(2):285–290, 1984. doi: 10.1115/1.3260906.

[29] H. Hayashi and S. Wada. Hydrodynamic lubrication of journal bearings by pseudo-plastic lubricants: Part 3, Theoretical analysis considering effects of correlation. *Bulletin of JSME* 17(109):967–974, 1974. doi: 10.1299/jsme1958.17.967.

[30] H. Hashimoto and S. Wada. The effects of fluid inertia forces in parallel circular squeeze film bearings lubricated with pseudo-plastic fluids. *Journal of Tribology*, 108(2):282–287, 1986. doi: 10.1115/1.3261177.

[31] J.-R. Lin. Non-Newtonian effects on the dynamic characteristics of one dimensional slider bearings: Rabinowitsch fluid model. *Tribology Letters*, 10:237–243, 2001. doi: 10.1023/A:1016678208150.

[32] U.P. Singh, R.S. Gupta, and V.K. Kapur. Effects of inertia in the steady state pressurised flow of a non-Newtonian fluid between two curvilinear surfaces of revolution: Rabinowitsch fluid model. *Chemical and Process Engineering*, 32(4):333–349, 2011. doi: 10.2478/v10176-011-0027-1.

[33] J.R. Lin. Non-Newtonian squeeze film characteristics between parallel annular disks: Rabinowitsch fluid model. *Tribology International*, 52:190–194, 2012. doi: 10.1016/j.triboint.2012.02.017.

[34] U.P. Singh. Application of Rabinowitsch fluid model to pivoted curved slider bearings. *Archive of Mechanical Engineering*, 60(2):247–266, 2013. doi: 10.2478/meceng-2013-0016.

[35] U.P. Singh and R.S. Gupta. Dynamic performance characteristics of a curved slider bearing operating with ferrofluids. *Advances in Tribology*, 2012:1–6, 2012. doi: 10.1155/2012/278723.

[36] U.P. Singh, R.S. Gupta, and V.K. Kapur. On the squeeze film characteristics between a long cylinder and a flat plate: Rabinowitsch model. *Proceedings of the Institution of Mechanical Engineers, Part J: Journal of Engineering Tribology*, 227(1):34–42, 2013. doi: 10.1177/1350650112458742.

[37] S.C. Sharma and S.K. Yadav. Performance of hydrostatic circular thrust pad bearing operating with Rabinowitsch fluid model. *Proceedings of the Institution of Mechanical Engineers, Part J: Journal of Engineering Tribology*, 227(11):1272–1284, 2013. doi: 10.1177/1350650113490147.

[38] Y. Huang and Z. Tian. A new derivation to study the steady performance of hydrostatic thrust bearing: Rabinowitch fluid model. *Journal of Non-Newtonian Fluid Mechanics*, 246:31–35, 2017. doi: 10.1016/j.jnnfm.2017.04.012.

[39] U.P. Singh, P. Sinha, and M. Kumar. Analysis of hydrostatic rough thrust bearing lubricated with Rabinowitsch fluid considering fluid inertia in supply region. *Proceedings of the Institution of Mechanical Engineers, Part J: Journal of Engineering Tibology*, 235(2):386–395, 2021. doi: 10.1177/1350650120945887.

[40] A. Cameron. *Basic Lubrication Theory*, 3rd edition. E. Horwood, 1981.